Mixing State of 1-Propanol Aqueous Solutions Studied by Small-Angle X-Ray Scattering: A New Parameter Reflecting the Shape of SAXS Curve

Hisashi HAYASHI[†,††] and Yasuo UDAGAWA*[,††]

[†] The Graduate University for Advanced Studies, Myodaiji, Okazaki, Aichi 444

[††] Research Institute for Scientific Measurements, Tohoku University, Katahira 2-1-1, Aobaku, Sendai 980

(Received August 2, 1991)

Small-Angle X-ray Scattering (SAXS) of 1-propanol aqueous solutions was measured at various temperatures with a newly constructed point-focusing diffractometer. Owing to the improvement of the SAXS data, it is now possible to accurately determine the higher order coefficients in a polynomial expansion. Accordingly, a new parameter which reflects the shape of the SAXS curve (χ) is proposed. The mixing states of 1-propanol aqueous solutions are discussed in terms of χ as well as the concentration fluctuation and correlation length which are also derived from SAXS measurements. Every obtained result implies that the mixing state of the solution changes very much above and below a concentration of about 15 mol%, and that the new parameter (χ) is very effective as an indicator.

For understanding the mixing states of aqueous solutions, a study of microinhomogeneities in a liquid is both useful and effective. A small-angle X-ray scattering (SAXS) measurement is one of the most direct ways to study microinhomogeneity. For small scattering angles, the SAXS intensity curve from an isotropic sample ($I(s)$) can be approximated by the following polynomial:[1)]

$$I(s)=r_0-r_2s^2+r_4s^4-r_6s^6+\cdots, \quad (1)$$

where

$$r_{2i}=(1/(2i+1)!)\int<\Delta\rho_e(0)\Delta\rho_e(r)>r^{2i}4\pi r^2dr. \quad (2)$$

Here, s is the scattering parameter ($s=4\pi\sin\theta/\lambda$ 2θ: scattering angle, λ: wavelength of X-rays), $\Delta\rho_e(r)$ is the difference in the electron density from the average at position r, and $<\cdots>$ denotes the ensemble average. The 'moment' determined through a SAXS measurement (r_{2i}) reflects the various properties of the solution. The zero-angle scattering ($I(0)$), which indicates the square of the number of molecules concerning the microinhomogeneity, is equal to r_0. The concentration fluctuation[2-4)] and Kirkwood–Buff parameters[5)] are derived from $I(0)$.[6)] The Debye's correlation length[7)] (L_D), which indicates the average size of the fluctuating structure, is defined by

$$L_D=(3!\cdot r_2/r_0)^{0.5}. \quad (3)$$

Previous SAXS studies have drawn conclusions only from r_0 and r_2, *i.e.*, $I(0)$ and L_D.

Recently, we constructed a point-focusing SAXS diffractometer.[8)] Owing to an improvement in the intensity and resolution, it is now possible to accurately determine higher order coefficients in the polynomial expansion shown in Eq. 1. Accordingly, a new parameter χ is proposed here. The χ is defined as

$$\chi=r_0\cdot r_4/r_2^2. \quad (4)$$

This dimensionless parameter reflects the shape of the SAXS curve, as will be discussed later.

A 1-propanol (abbreviated to NPA, hereafter) aqueous solution is one of the most notable systems in studying mixing states; this solution has no critical temperature, in spite of its large microinhomogeneity. Recently, several measurements of the microinhomogeneity in this solution have been performed using different techniques: ultrasonic absorption,[9)] light scattering,[10)] small-angle neutron scattering (SANS),[11)] and small-angle X-ray scattering (SAXS).[2)] Details are, however, not clear as of yet. This is in part due to either the insufficient range of the concentration and temperature employed in previous studies, or to a lack of measures of microinhomogeneity. In this paper, the mixing state of an NPA aqueous solution is, accordingly, discussed in terms of the concentration fluctuation and correlation length, as well as χ, derived from SAXS data obtained for wide concentration and temperature ranges.

Experimental

NPA aqueous solutions of the following concentrations were prepared by weighing the components: C_1=0.051, 0.071, 0.089, 0.111, 0.122, 0.137, 0.167, 0.200, 0.253, and 0.299. Here, C_1 indicates the mole fraction of NPA. The water used for the preparation was deionized and distilled. NPA of reagent grade with a 99.9% specified purity was used after drying with molecular sieves (3A 1/8, Aldrich). Each sample was kept in a cell with about 0.1 mm-thick mica windows. The thickness of the sample was 2.5 mm.

Measurements of the SAXS on each sample were performed at 15, 25, 35, and 40 °C. The temperature of each sample was kept constant within 0.5 °C by using a cell holder coupled to a bath circulator.

A diffractometer with a double-bent LiF crystal monochromator[8)] was used for the SAXS measurements. Scattered X-rays were detected by a position-sensitive proportional counter (PSPC). The details are described in Ref. 8. The s-region (ranging from 0.03 to 0.40 Å^{-1}) is covered by this diffractometer. The accumulation times for samples were 10000—20000 s.

Data Treatment

The data were corrected for background scattering, multiple scattering, Compton scattering, and absorption.[8] They were, subsequently, converted into an absolute scale by using the value obtained from the calibration of SAXS about water, methanol, and NPA.[8]

The SAXS curve ($I(s)$) can generally be approximated by the following Ornstein–Zernike equation $I_{OZ}(s)$ for $\xi s \ll 1$:[12]

$$I_{OZ}(s) = I(0)/(1+(\xi s)^2). \quad (5)$$

Here, ξ is the so-called correlation length,[12] which is related to Debye's correlation length (L_D) by $\xi = L_D/6^{0.5}$.[4] Thus, $I(0)$ and ξ can be determined from a plot of $I^{-1}(s)$ vs. s^2, an Ornstein–Zernike plot.[11]

$$I^{-1}(s) = 1/I(0) + (\xi^2/I(0))s^2, \quad (6)$$

Then, each $I(s)$ in the region $\xi/s < 0.8$ was approximated by using Eq. 1, and the coefficients (r_{2i}) were determined by a least-squares calculation. The R-factor defined in the following equation did not exceed 0.0001 in all data:

$$R = \Sigma(I^{obsd} - I^{calcd})^2/\Sigma(I^{obsd})^2. \quad (7)$$

Here, I^{obsd} is the measured intensity and I^{calcd} is the intensity calculated by Eq. 1. From these r_{2i}, χ was calculated according to Eq. 3.

Results

The temperature dependence of $I(0)$ is shown in Fig. 1. The magnitude of the error in the $I(0)$ value was estimated to be 3%. By using $I(0)$, together with the isothermal compressibility and partial molar volumes, the mean square fluctuation in concentration $\langle N\rangle\langle(\Delta C_1)^2\rangle$ shown in Fig. 2 and other fluctuation parameters could be obtained, as was described previously.[6] Here, N is the total particle number. The phrase "mean square" is omitted hereafter. The partial molar volumes and isothermal compressibilities at 15, 25, and 35 °C were calculated from the data of Benson and Kiyohara.[13–15] The fluctuation parameters at 40 °C were not obtained because of a lack of data concerning the partial molar volumes. The total magnitude of the error in the concentration fluctuation was estimated to be 5%.

The temperature dependence of ξ and that of χ are shown in Figs. 3 and 4, respectively. The ξ value calculated from SANS data[11] (for C_1=0.114, at 25 °C), which is in good agreement with ours, is also shown in Fig. 3.

$\langle N\rangle\langle(\Delta C_1)^2\rangle$ shows no marked temperature dependence and varies with the concentration, having a maximum at about 20 mol%. ξ is essentially independent of the temperature and varies only slightly with the concentration, having a maximum at about 15 mol%. On the other hand, χ depends on both the temperature

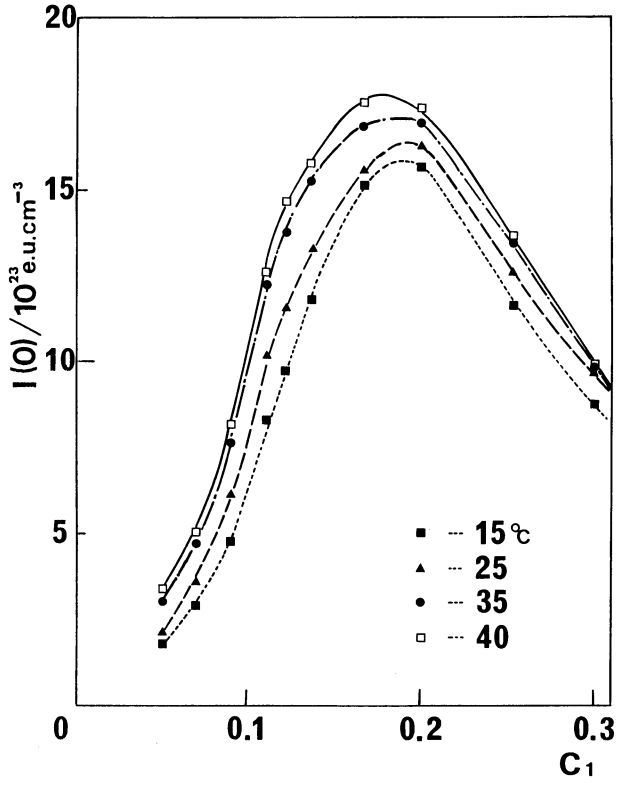

Fig. 1. Temperature dependence of the zero-angle X-ray scattering intensity against the mole fraction of NPA (C_1).

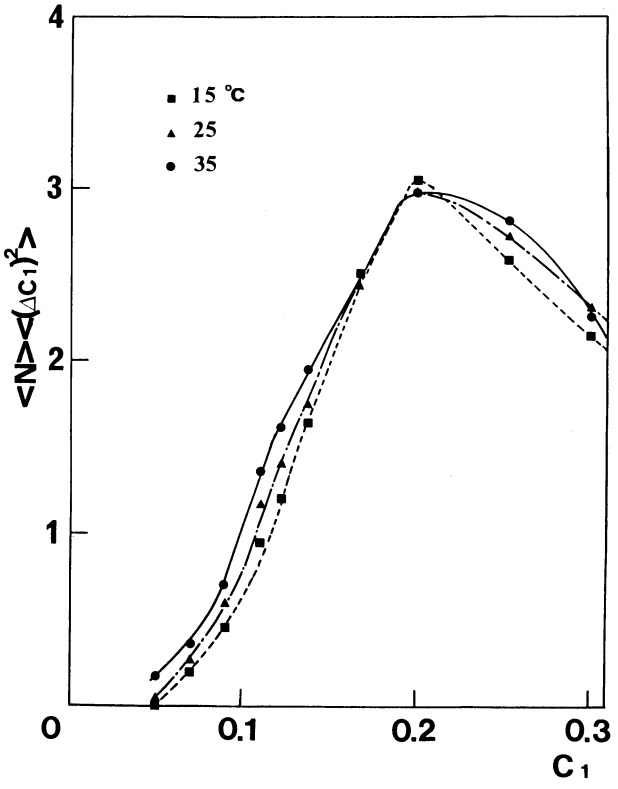

Fig. 2. Temperature dependence of the concentration fluctuation of NPA aqueous solutions.

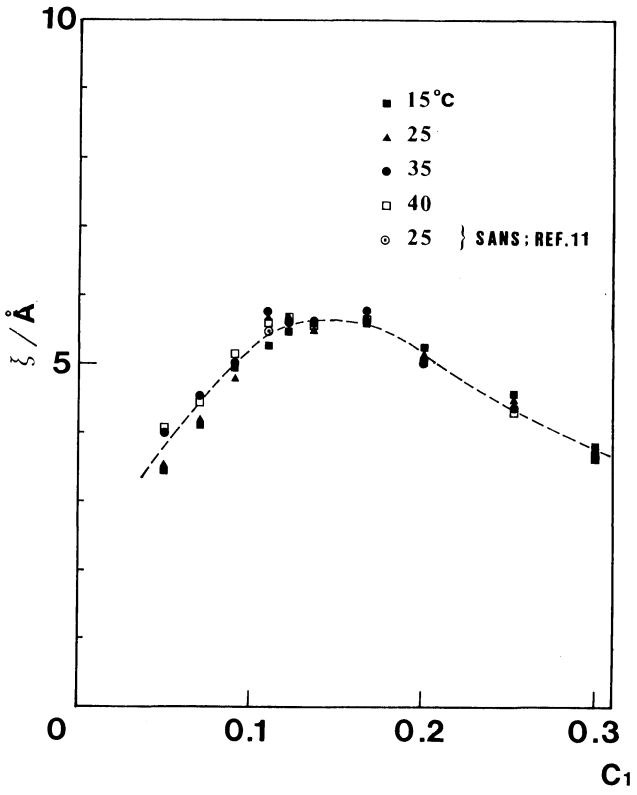

Fig. 3. Temperature dependence of the correlation length (ξ) against the mole fraction of NPA (C_1).

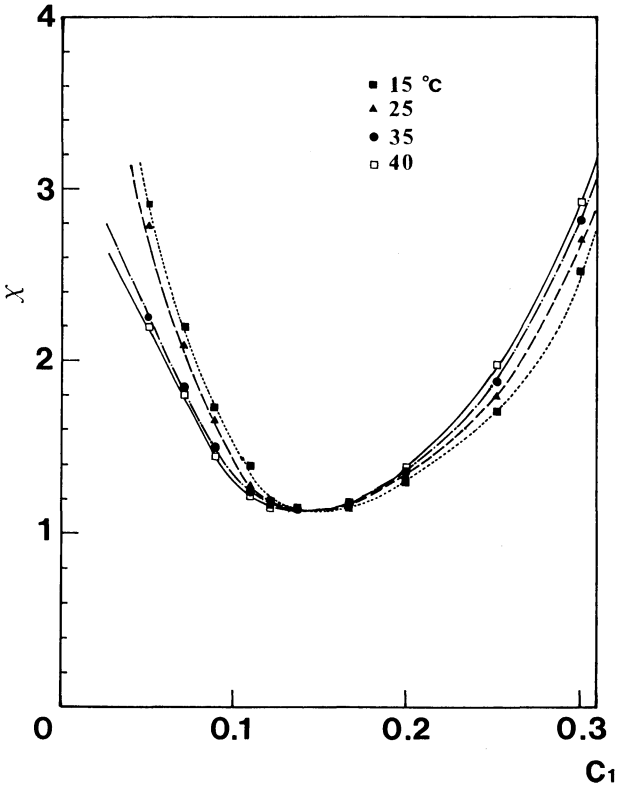

Fig. 4. Temperature dependence of parameter χ against the mole fraction of NPA (C_1).

and concentration, and shows a different temperature dependence at higher and lower concentrations. Hence, NPA aqueous solutions can be classified by using χ into the following three concentration regions:

(a) C_{low}: ($C_1<0.12$). In this concentration region, the χ-values are relatively large and *decrease* sharply with either an increase in the temperature or concentration.

(b) C_{middle}: ($0.12<C_1<0.20$). In this concentration region, the χ-values are relatively small, and depend little on the temperature and concentration. $<N><(\Delta C_1)^2>$ and ξ take maximum values at each temperature in this region.

(c) C_{high}: ($C_1>0.20$). In this concentration region, the χ-values are relatively large and *increase* sharply with either an increase in the temperature or concentration.

Discussion

Physical Meaning of χ. Being related to r_4, χ reflects the shape of $I(s)$. To understand the physical meaning of χ further, let us examine the following theoretical SAXS functions: The exact function for spheres with a uniform size dispersed in a continuous medium ($I_s(s)$), the Guinier function ($I_G(s)$), and $I_{OZ}(s)$ (Eq. 5). Here, $I_G(s)$ is an approximate function for particles characterized by the radius of gyration (R_G). $I_s(s)$ and $I_G(s)$ are commonly employed for analyses of SAXS from colloidal or micellar systems and $I_{OZ}(s)$ for that from critical solutions. $I_s(s)$ is as follows:[1)]

$$I_s(s) = I(0)[3\{\sin(sR_0) - (sR_0)\cos(sR_0)\}/(sR_0)^3]^2, \quad (8)$$

where R_0 is the radius of the sphere. $I_G(s)$ is as follows:[1)]

$$I_G(s) = I(0)\exp(-R_G^2 s^2/3). \quad (9)$$

$I_s(s)$ can be expanded for $sR_0<1$ as

$$I_s(s) \propto 1 - (R_0^2/5)s^2 + (19R_0^4/1400)s^4 - \cdots. \quad (10)$$

The χ of $I_s(s)$ is, thereby, 19·25/1400, about 0.34. Being Lorentzian and Gaussian, the χ of Eqs. 5 and 9 are 1.0 and 0.5, respectively.

It should be mentioned here that an analysis by a polynomial expansion and by χ is valid only for $s^2(r_2/r_0) = s^2\xi^2<1$. Since the maximum $s\xi$ is 0.8 in the present case, the use of Eq. 1 is justified.

The correlation functions for $I_s(s)$, $I_G(s)$, and $I_{OZ}(s)$ can be expressed analytically as follows:[1,12)]

$$<\Delta\rho_e(0)\Delta\rho_e(r)>_s \propto 1 - (3/2)(r/2R_0) + (1/2)(r/2R_0)^3, \quad (11)$$

$$<\Delta\rho_e(0)\Delta\rho_e(r)>_G \propto \exp[-3r^2/(2R_G)^2], \quad (12)$$

and

$$<\Delta\rho_e(0)\Delta\rho_e(r)>_{OZ} \propto \exp(-r/\xi)/r. \quad (13)$$

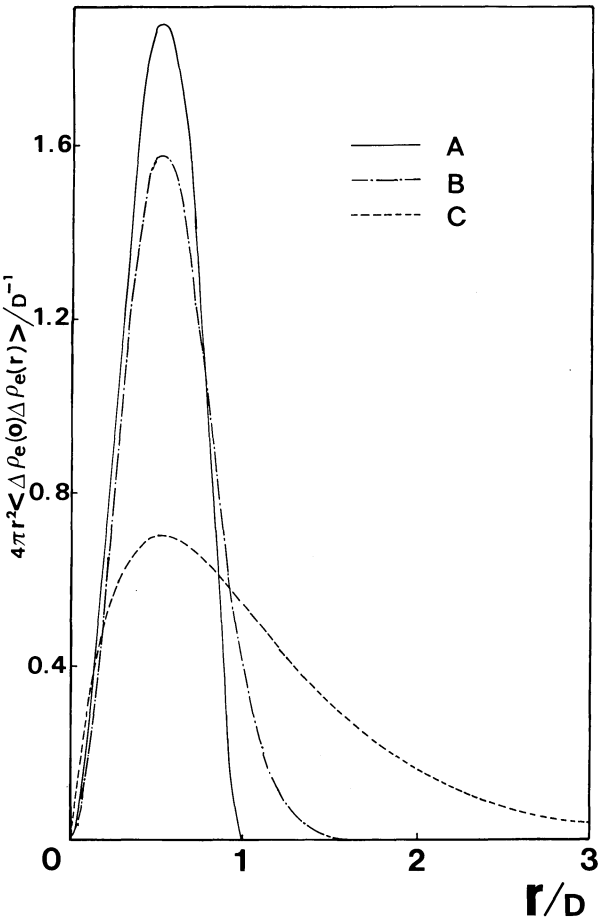

Fig. 5. Theoretical correlation functions. A, B, and C show $4\pi r^2<\Delta\rho_e(0)\Delta\rho_e(r)>_S$, $4\pi r^2<\Delta\rho_e(0)\Delta\rho_e(r)>_G$, and $4\pi r^2<\Delta\rho_e(0)\Delta\rho_e(r)>_{OZ}$, respectively. Here, D is the diameter of a sphere: $D=2R_0$.

They are shown in Fig. 5 in the form of $4\pi r^2<\Delta\rho_e(0)\Delta\rho_e(r)>$. $4\pi r^2<\Delta\rho_e(0)\Delta\rho_e(r)>_S$ has a maximum at $(r/2R_0)\simeq0.525$, $4\pi r^2<\Delta\rho_e(0)\Delta\rho_e(r)>_G$ at $r=(4/3)^{0.5}R_G$, and $4\pi r^2<\Delta\rho_e(0)\Delta\rho_e(r)>_{OZ}$ at $r=\xi$. The values of R_G and ξ in Fig. 5 were determined in such a way that the positions of the maxima are the same.

The difference among these functions lies in the decay at large r, as observed in Fig. 5. Here, the steep/gradual decay curve of the correlation functions should represent the clear/obscure boundary of the fluctuating structure. Since $\chi=0.34$ for $I_S(s)$, $\chi=0.5$ for $I_G(s)$, and $\chi=1.0$ for $I_{OZ}(s)$, χ serves as an indicator of the sharpness of the boundary. The physical meaning of the boundary of the spheres is self-evident, and that of the structures expressed by Eqs. 5 and 9, corresponds to the size-dispersion of aggregates or clusters formed in solution. Hence, χ can be regarded as being an indicator for the size-dispersion of clusters: a large/small χ value indicates a large/small size-dispersion of the clusters in solution.

Mixing State of NPA Aqueous Solutions. As described previously, the mixing states of NPA aqueous solutions can be classified by χ into three regions: C_{low}, C_{middle}, and C_{high}.

In the C_{middle} region, $<N><(\Delta C_1)^2>$ and ξ show maxima and χ takes a minimum, suggesting that the microinhomogeneity is large and has a sharp boundary. Hence, the formation of some kind of aggregates is expected.

A large microinhomogeneity characterized by a large concentration fluctuation and long correlation length has been observed in several aqueous solutions of nonionic amphiphiles with relatively short tail, e.g. NPA,[2,9-11] *t*-butyl alcohol (TBA),[16-18] 2-butoxyethanol (BE),[11,19,20] and tetrahydrofuran (THF).[21] The mixing states of these solutions have been described by assuming either clathrate hydrate-like aggregates (TBA, BE, and THF) or micelle-like aggregates (NPA and BE); such aggregates must also be the origin of the observed microinhomogeneity in NPA.

Although it is not possible to determine which is the case for the NPA solution, a micelle-like aggregate is more likely than a clathrate hydrate, because of the molecular structure; the hydrophobic tail of NPA without branch should work effectively for a hydrophobic interaction, while a large distortion of the hydrogen bond is required if an NPA molecule is caged by water molecules.[2]

Grossmann and Ebert (GE) found that various physical properties, such as the translational diffusion constant and the hydrodynamic radius of a cluster, show either a maximum or minimum at a molar ratio of 1 NPA and 5 water (ca. 17 mol%), and proposed the existence of micelle-like aggregates comprising $(n\text{-}C_3H_7OH)_8(H_2O)_{40}$, and having a diameter of 16 Å.[10] Although this model is considered to be qualitatively correct, it should be revised in view of the present SAXS study, for the following reasons. First, although the formation of aggregates of uniform size proposed by GE must lead to an extremely small concentration fluctuation,[2] the fluctuation is experimentally fairly large, and close to the maximum at this concentration, as is shown in Fig. 2. Second, the χ value is about 1.1, suggesting that the sizes of aggregates are not uniform. For a system comprising spheres of uniform size dispersed in a continuous medium, χ was calculated to be 0.34 (as described previously). For an analysis of $I(s)$ from micellar systems, $I_G(s)$ is usually used;[1] in this case χ is 0.5, which is still much smaller than the observed value, 1.1. Thus, size-dispersion among micelle-like aggregates is concluded in the NPA solution in the C_{middle} region; it should be much larger than that of ordinary micelles.

The temperature dependence of an aggregate near NPA 17 mol% is somewhat peculiar. Micelles of nonionic amphiphile are known to grow in size with a temperature rise,[22] and aggregates of nonionic amphiphiles such as BE, TBA, and THF are reported to behave in a similar fashion.[11,16-21] However, no marked temperature dependence of $<N><(\Delta C_1)^2>$ and of ξ has

been observed near NPA 17 mol%, as shown in Figs. 2 and 3. In accordance with the present observation, GE also observed that the hydrodynamic radius is essentially independent of the temperature.[10] The reason for this lack of a marked temperature dependence is not clear.

In the C_{low} region, $<N><(\Delta C_1)^2>$ and ξ increase with an increase in the concentration. This is very similar to that observed with other aqueous solutions of amphiphiles and indicates the growth of (probably micelle-like) aggregates.[2,4,16-18] The χ values in C_{low} decrease with an increase in the concentration, also suggesting the formation of aggregates with certain sizes.

In the C_{high} region, $<N><(\Delta C_1)^2>$ and ξ decrease with an increase in the concentration; χ also increases. This means that the aggregates in C_{high} become smaller and the size distribution wider with the concentration. This must be due to an insufficiency in the number of water molecules available to form stable micelle-like aggregates consisting of, on the average, a molar ratio of 1 NPA to 5 H_2O.

On the other hand, there are surplus water molecules in the C_{low} region. $<N><(\Delta C_1)^2>$ is much smaller in C_{low} than in C_{high}, as shown in Fig. 2. This indicates that the aggregates in C_{high} should not be the same as that in C_{low}, and that the number of water molecules forming aggregates in C_{high} is larger than that in C_{low}. The temperature dependence of χ in C_{high} is opposite to that in C_{low}, as shown in Fig. 4, which also indicates a difference of the aggregates.

In conclusion, a new parameter (χ) which reflects the shape of $I(s)$ has been found to be a good indicator of microinhomogeneity in solution. By means of χ, the mixing states of NPA aqueous solutions can be classified into three regions, and the large microinhomogeneity near NPA 17 mol% is attributed to the formation of micelle-like aggregates.

The authors thank Dr. K. Nishikawa at Yokohama National University for helpful discussions.

References

1) G. Porod, "Small Angle X-Ray Scattering," ed by O. Glatter and O. Kratky, Academic Press, London (1982), p. 17.
2) H. Hayashi, K. Nishikawa, and T. Iijima, *J. Phys. Chem.*, **94**, 8334 (1990).
3) K. Nishikawa, Y. Kodera, and T. Iijima, *J. Phys. Chem.*, **91**, 3694 (1987).
4) K. Nishikawa, H. Hayashi, and T. Iijima, *J. Phys. Chem.*, **93**, 6559 (1989).
5) J. G. Kirkwood and F. P. Buff, *J. Chem. Phys.*, **19**, 774 (1951).
6) H. Hayashi, K. Nishikawa, and T. Iijima, *J. Appl. Crystallogr.*, **23**, 134 (1990).
7) P. Debye, *J. Chem. Phys.*, **31**, 680 (1959).
8) H. Hayashi, K. Tohji, and Y. Udagawa, *Jpn. J. Appl. Phys.*, **30**, 870 (1991).
9) W. M. Madigosky and R. W. Warfield, *J. Chem. Phys.*, **86**, 1491 (1987).
10) G. H. Grossmann and K. H. Ebert, *Ber. Bunsen-Ges. Phys. Chem.*, **85**, 1026 (1981).
11) G. D'Arrigo and J. Teixeira, *J. Chem. Soc., Faraday* Trans., **86**, 1503 (1990).
12) J. M. Ziman, "Models of Disorder," Cambridge University Press, Cambridge (1979).
13) G. C. Benson and O. Kiyohara, *J. Solution Chem.*, **9**, 791 (1980).
14) G. C. Benson, P. J. D'Arcy, and O. Kiyohara, *J. Solution Chem.*, **9**, 931 (1980).
15) O. Kiyohara and G. C. Benson, *J. Solution Chem.*, **10**, 281 (1981).
16) Y. Koga, *Chem. Phys. Lett.*, **111**, 176 (1984).
17) K. Iwasaki and T. Fujiyama, *J. Phys. Chem.*, **81**, 1908 (1977); **83**, 463 (1979).
18) G. W. Euliss and C. M. Sorensen, *J. Chem. Phys.*, **80**, 4767 (1984).
19) G. Roux, G. Perron, and J. E. Desnoyers, *J. Phys. Chem.*, **82**, 966 (1978).
20) Y. Koga, W. W. Y. Siu, and T. Y. H. Wong, *J. Phys. Chem.*, **94**, 3879 (1990).
21) C. M. Sorensen, *J. Phys. Chem.*, **92**, 2367 (1988).
22) C. Tanford, "The Hydrophobic Effect," Wiley, New York (1980).